PNAS RESEARCH ARTICLE | APPLIED PHYSICAL SCIENCES

# Receptor clustering tunes and sharpens the selectivity of multivalent binding

Zhaoping Xie[a], Stefano Angioletti-Uberti[b], Jure Dobnikar[c,d,e], Daan Frenkel[f], and Tine Curk[g,1]

Edited by Monica Olvera de la Cruz, Northwestern University, Evanston, IL; received August 23, 2024; accepted January 11, 2025

**The immune system exploits a wide range of strategies to combine sensitivity with selectivity for optimal response. We propose a generic physical mechanism that allows tuning the location and steepness of the response threshold of cellular processes activated by multivalent binding. The mechanism is based on the possibility to modulate the attraction between membrane receptors. We use theory and simulations to show how tuning interreceptor attraction can enhance or suppress the binding of multivalent ligand-coated particles to surfaces. The changes in the interreceptor attraction less than the thermal energy $k_BT$ can selectively switch the receptor-clustering and activation on or off in an almost step-wise fashion, which we explain by near-critical receptor density fluctuations. We also show that the same mechanism can efficiently regulate the onset of endocytosis for, e.g., drug delivery vehicles.**

multivalent binding | receptor clustering | superselectivity | Monte Carlo

## Significance

Organisms must be able to distinguish between harmful and harmless external agents. A failure to mount a cellular response to an attack can be life-threatening, but so is an incorrect response (e.g., an autoimmune reaction). Discrimination between "dangerous" and "safe" situations requires the existence of a sharp and precisely located threshold where the response changes almost stepwise from no response to full response. We demonstrate a general mechanism based on modulating receptor–receptor interactions that allows cells to tune the response threshold to external agents.

Clustering of receptors on a cellular membrane due to binding of an external agent is associated with a wide range of biological processes, from activation of the immune system to the receptor-mediated endocytosis and exocytosis that regulates the transport of vesicles, viruses, and nanoparticles in the cellular environment (1). Because these processes are implicated in cellular responses that are crucial for the survival of an organism, tight control of their activation is needed.

Clustering may have different effects, such as the enhanced propensity for the clustered molecules to be "activated" (2, 3) or to regulate transmembrane signaling (4). A key question is how the system can be tuned such that there is a sharp threshold for clustering and subsequent activation. The tendency of receptor-cluster formation depends on control parameters such as the strength of the interreceptor attraction, the temperature, the pH, or the presence of other molecular species, e.g., adaptor proteins (5–7). The response to these control parameters should exhibit a sharp threshold. It is an open question by what physical mechanism or mechanisms a cell can achieve a sharp onset of receptor clustering, i.e., high selectivity.

Here, we focus on receptor clustering induced by reversible binding to an external multivalent agent ("vector"), e.g., a nanoparticle or a virus, that binds to a set of multiple receptors and refer to this specific binding modality as activation. Molecular specificity of ligand–receptor pairs is a necessary condition to obtain controlled activation but is not sufficient. The existence of a sharp onset for vector binding can be accounted for by so-called multivalent superselectivity. Superselective binding of multivalent moieties to surfaces such as cell membranes has been studied theoretically, numerically, and experimentally (8–11). However, a sharp and strong superselective response only occurs in a narrow range of control parameters, which may be difficult to achieve. For example, for a fixed ligand–receptor bond strength and density of the cognate ligands on the multivalent agent, binding only shows a sharp response around a specific density of membrane receptors. This threshold receptor density would be fixed by the chemical nature of the receptor–ligand bond, whereas in reality, cells can tune their response to external agents: They seem to be able to control their sensitivity to the external signal.

One could argue that cells achieve this control by regulating the expression of different membrane receptors, or by modifying the ligand-binding epitope of existing ones. For example, by modifying the binding of CD44 receptors to hyaluronic acid via glycosylation (12). Notably, this strategy would require replacing existing membrane receptors with new ones, a slow and inefficient process, and would need to be precisely tailored for each specific ligand. Even if such fine chemical tuning was possible, multivalent superselectivity has additional constraints; it is usually confined to processes with relatively large threshold concentration of receptors (9–11). It would seem fairly inefficient to maintain a large receptor concentration everywhere on a cell membrane to enable local binding to a multivalent entity. This raises the question whether there is a

Author affiliations: [a]Department of Genetic Medicine, Johns Hopkins University School of Medicine, Baltimore, MD 21205; [b]Department of Materials, Imperial College London, London SW7 2AZ, United Kingdom; [c]Chinese Academy of Sciences Key Laboratory of Soft Matter Physics, Institute of Physics, Chinese Academy of Sciences, Beijing 100190, China; [d]School of Physical Sciences, University of Chinese Academy of Sciences, Beijing 100049, China; [e]Wenzhou Institute, University of Chinese Academy of Sciences, Wenzhou, Zhejiang 325011, China; [f]Department of Chemistry, University of Cambridge, Cambridge CB2 1EW, United Kingdom; and [g]Department of Materials Science and Engineering, Johns Hopkins University, Baltimore, MD 21218

Author contributions: T.C. designed research; Z.X. and S.A.-U. performed research; Z.X., S.A.-U., J.D., D.F., and T.C. analyzed data; and Z.X., S.A.-U., J.D., D.F., and T.C. wrote the paper.

The authors declare no competing interest.

This article is a PNAS Direct Submission.



[1]To whom correspondence may be addressed. Email: tcurk@jhu.edu.

Published XXXX.

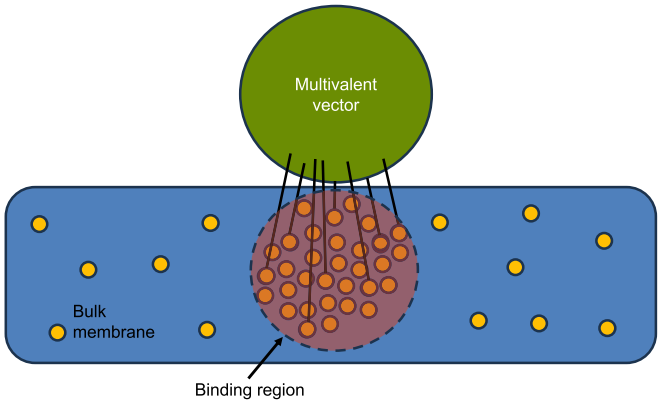


**Fig. 1.** Schematic representation of the system. A multivalent nanoparticle or vector (green) with ligands (black lines) on top of a cell membrane (blue) in which receptors (orange) can move freely. Ligand–receptor bonds can form in the local binding region (dashed transparent red), where the local density of receptors is higher than in the rest of the membrane and potentially closer to an instability with respect to a gas–liquid phase separation.

way to obtain a sharp, superselective response that can be tuned over a broad range of receptor densities?

## 1. Hypothesis

We assume that specific, although not necessarily strong, ligand–receptor interactions exist, and we focus on the question of what generic physical mechanisms could be used to both tune and sharpen the response threshold. We hypothesize that the up- or down-regulation of weak, nonspecific interreceptor interactions in combination with multivalent binding to the external nanoparticle or a vector provides such a mechanism. The mechanism that we describe is based on statistical mechanics of phase separation and critical fluctuations and can play a role whenever induced clustering of receptors is involved; see Fig. 1. We stress that although sharp activation is highly desirable, it would be of limited use if the activation threshold cannot be tuned. It is precisely the control of the interactions between membrane receptors that can play this "tuning" role. Receptor–receptor interactions can be controlled, for example, through phosphorylation (3) or binding of adaptor proteins (5–7).

In the following, we provide numerical evidence that the mechanism we just described indeed enables tunability and can lead to a giant enhancement in binding selectivity to changes in various control parameters. For the sake of generality, we show this first for a lattice model of multivalent binding and provide a general quantitative theoretical argument. We then apply the findings to demonstrate tunability in ligand–receptor-mediated endocytosis.

## 2. Lattice Model

To investigate the role of receptor–receptor interactions on the selectivity of binding, we consider the binding of a multivalent particle or a vector to the cell membrane. An example of practical importance is a ligand-functionalized drug-delivery nanoparticle interacting with the membrane of a cancer cell through the cognate receptors (13). A natural equivalent would be viral attachment to the cell membrane, which is the initial step of an infection (14, 15). A general lattice model that captures these scenarios is depicted in Fig. 2 *A* and *B*. To keep a general scope, we use the term "'receptor" for any membrane-bound entity, for example, membrane proteins, biological receptors, or specific lipids, that bind to the multivalent agent. A membrane contains mobile receptors at surface number density $\sigma$. Each receptor can occupy one lattice site and can interact with neighboring receptors with energy $\varepsilon_{rr}$ [a lattice gas model (16)]. Multivalent guest particles at chemical potential $\mu_p$ can bind to the membrane via binding to receptors with interaction energy $\varepsilon_{pr}$ per particle–receptor bond. The area "footprint" per receptor is $b$, and the size of the multivalent particles is $k$, which denotes the valency, i.e., the maximum number of receptors that a particle can bind to. Additionally, we assume that ligands, or receptors, are sufficiently flexible (Fig. 2*A*) so that different ligands can bind independently, i.e., $\varepsilon_{pr}$ is the same for all ligands. We employ grand-canonical Monte Carlo simulations to compute the equilibrium surface fraction of the adsorbed particles $\theta = \langle N_p \rangle k/M$, with $\langle N_p \rangle$ the

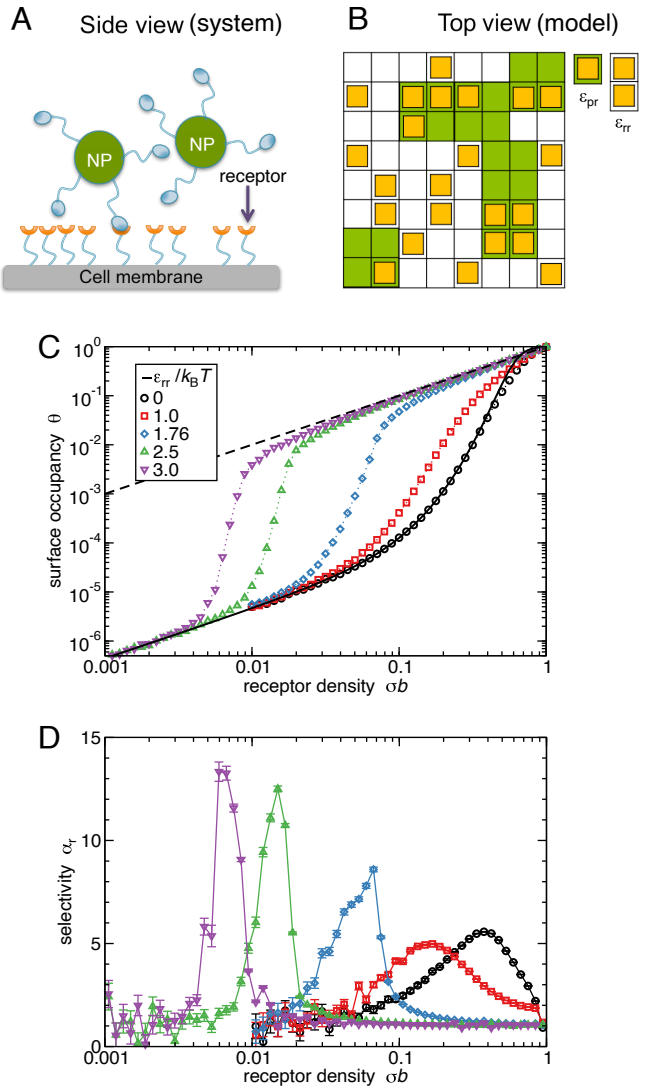


**Fig. 2.** Receptor–receptor attraction increases the selectivity. (*A* and *B*) Schematic of the system (*A*) and the lattice model (*B*). The receptors (orange) are described as a lattice gas with nearest-neighbor interaction $\varepsilon_{rr}$. Each guest particle (green), here represented as a 2 × 2 square, occupies $k$ lattice sites and interacts with up to $k$ receptors with an energy $\varepsilon_{pr}$. (*C* and *D*) Surface occupancy $\theta$ and corresponding selectivity $\alpha_r$ (Eq. **1**) from MC simulations showing the effect of receptor–receptor attraction. The solid black line shows the theoretical prediction for $\varepsilon_{rr} = 0$ (see *Materials and Methods*, Eqs. **11** and **13**) and the dashed line, $\theta = \sigma b$, shows the opposite, strong binding limit $-\varepsilon_{rr} \gg k_BT$. Parameters: $\mu_p = -11.5k_BT$, $\varepsilon_{pr} = -k_BT$, $k = 4 \times 4 = 16$, and $M = 80 \times 80$.

average number of particles attached to the membrane, $k$ the size (valency) of each particle and $M$ the total number of lattice sites.

Employing the lattice model, we calculate the adsorption profiles for different receptor densities and receptor–receptor interactions; see Fig. 2*C*, which demonstrates that the introduction of interreceptor attraction not only tunes the binding threshold but also strongly enhances the binding selectivity. A convenient measure of selectivity to changes in receptor concentration is the parameter $\alpha_r$ defined as (9):

$$\alpha_r = \frac{d\ln\theta}{d\ln\sigma}, \qquad [1]$$

where the introduction of the logarithm in Eq. **1** is used to measure the fractional change of binding rather than its absolute value, which is particularly useful when one needs to measure a response to quantities that can take values across multiple orders of magnitude. Defined in this way, the value of $\alpha_r$ is also independent of units used to measure $\theta$ and $\sigma$. The binding response is called superselective when it is superlinear in receptor density, that is, when $\alpha_r > 1$. Theoretical predictions for $\alpha_r$ for various types of multivalent particles can be found in refs. 9–11, and 17.

As argued above, we should expect to achieve a large increase in selectivity when the receptors approach a condensation transition. For our lattice model, we can estimate that such a transition occurs when $\varepsilon_{rr} \le \varepsilon^*_{rr} = -2\log(1+\sqrt{2})\ k_BT \approx -1.76\,k_BT$, with $k_B$ the Boltzmann constant and $T$ the absolute temperature, which is the interaction strength at the critical point of the lattice gas model, equivalent to the Ising model (16). The MC simulations indeed show that the selectivity increases rapidly close to the critical point (Fig. 2*D*) and peaks at a value of $\alpha_r \approx 13$ for $\varepsilon_{rr} < \varepsilon^*_{rr}$. As can be seen from the figure, this implies that a 50% change in the receptor density causes a change of two orders of magnitude in the density of adsorbed particles. We can explain this enhancement by recognizing that receptor–receptor attraction makes the binding cooperative; once the first receptor binds, it becomes easier for the second to bind, etc. Cooperativity approaches an all-or-nothing binding for which $\alpha_r \to k$ (see *Materials and Methods*, Eq. **14**). Thus, we predict that for even stronger interaction, $\varepsilon_{rr} \ll \varepsilon^*_{rr}$, the selectivity would not increase further, but the location of the transition would shift to very low receptor densities. This is not desired because, as will be quantified below, low receptor density leads to slower condensation kinetics, slowing the response, and a too-low receptor count may become insufficient to trigger intracellular processes.

Sufficiently strong interactions between membrane lipids can cause (micro) phase separation and formation of so-called lipid rafts within the membrane (18–20). Here, we show that a sufficiently strong attraction between receptors can similarly cause receptor clustering provided the receptor density is above the critical concentration. In this case, however, the multivalent particles simply bind to the preformed clusters, for which the dependence on $\varepsilon_{rr}$ is lost while the dependence on $\sigma$ is linear (dashed line in Fig. 2*C*). Moreover, strong attraction can lead to undesirable kinetically arrested aggregates, which would decrease selectivity. Thus, phase separation of receptors in the membrane itself is not a desired feature, since it is detrimental both to tunability and selectivity of binding. In contrast, multivalent particles (large $k$) together with weak receptor–receptor interactions provide high selectivity and tunability. Although selectivity could be further increased by optimizing the interaction energies, critical interactions for the simple lattice gas model $\varepsilon^*_{rr}$ can be considered a good rule of thumb for achieving a sharp on/off binding response.

The enhanced response is general to other control parameters. For example, multivalency also induces a sharp response to changes in the bond strength $K = \exp\left(-\varepsilon_{pr}/k_BT\right)$, which is proportional to the ligand–receptor affinity $K_d$ but also includes entropic effect due to ligand flexibility (see e.g. ref. 11). It is therefore useful to generalize the concept of superselectivity to control parameters ($\gamma$) other than just the receptor concentration $\sigma$. For any control parameter $\gamma$, we can define a quantity $\alpha(\gamma)$, analogous to Eq. **1**, that measures the sharpness of the response as:

$$\alpha(\gamma) = \frac{d\ln\theta}{d\ln\gamma}. \qquad [2]$$

Practical choices of control parameters $\gamma$ could be the bond strength $K$, the concentrations of ions (such as $H^+$, i.e., the pH), or concentration of some molecular species in solution that can bind competitively to either ligands or receptors (21, 22). Whenever $\alpha(\gamma) > 1$, the multivalent binding to the target membrane is deemed to exhibit "generalized superselectivity."

To evaluate the ability of cells to tune binding via changing the receptor–receptor interaction, we here set $\gamma = K_{rr}$, with the equilibrium constant $K_{rr} = \exp[-\varepsilon_{rr}/k_BT]$. Lattice model results for two representative receptor densities show that $\theta$ indeed depends sensitively on $\varepsilon_{rr}$; changing $\varepsilon_{rr}$ by as little as $0.45\ k_BT$ (equivalent to a change in equilibrium constant $K_{rr}$ by a factor $\approx$1.6) yields a nearly two orders of magnitude change in the surface occupancy (Fig. 3). In this case, selectivity can be

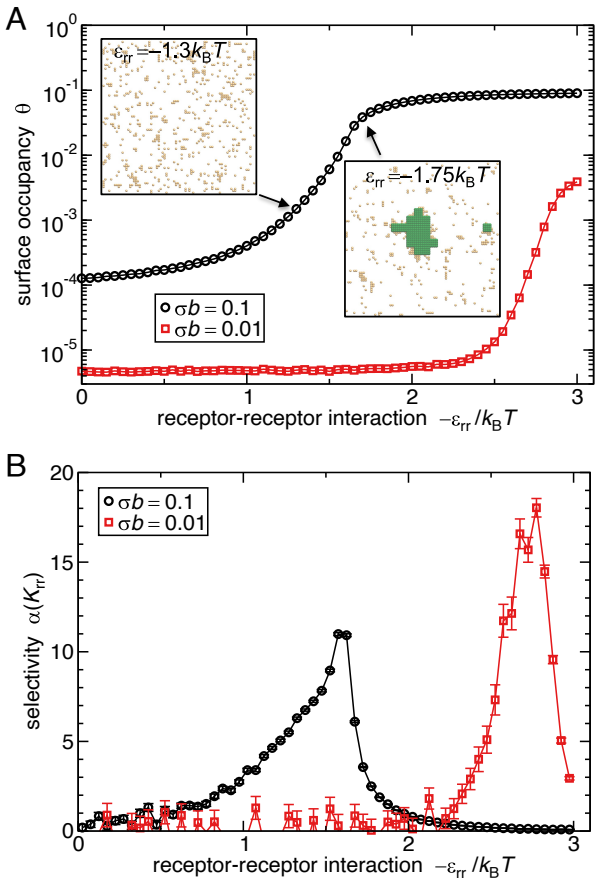


**Fig. 3.** Controlling binding via receptor–receptor interaction $\varepsilon_{rr}$. (*A*) Surface occupancy $\theta$ obtained from MC simulations and (*B*) corresponding selectivity $\alpha(K_{rr})$, Eq. **2**, with $K_{rr} = \exp(-\varepsilon_{rr}/k_BT)$. *Inset* in (*A*) shows representative configurations where orange spheres represent the receptors and green squares the nanoparticles (Fig. 2*B*). Parameters: $\mu_p = -11.5k_BT$, $\varepsilon_{pr} = -k_BT$, $k = 16$, and $M = 80 \times 80$.

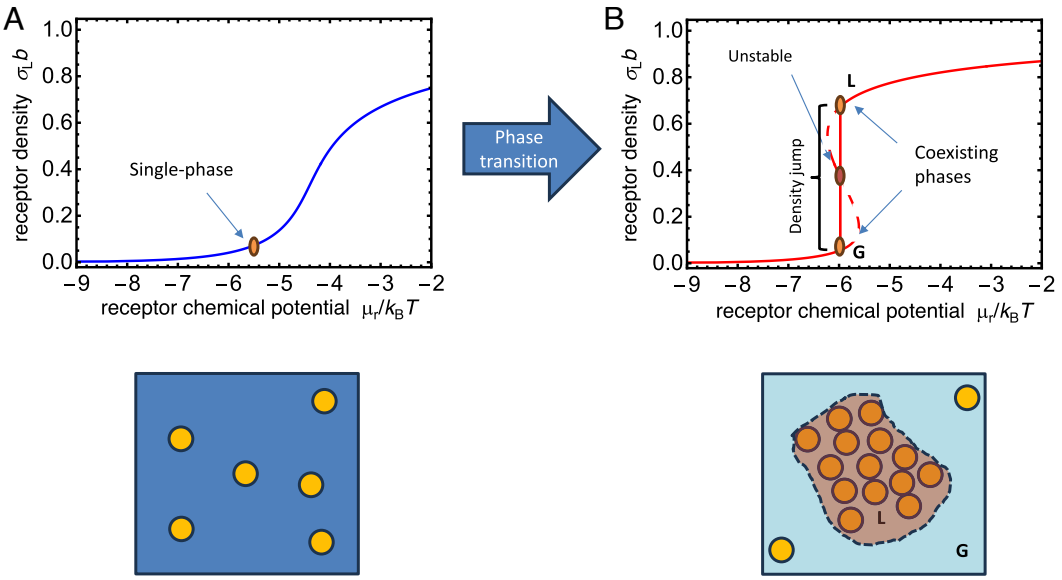


**Fig. 4.** Schematic of gas–liquid phase separation and its effect on selectivity. Local receptor density dependence on the chemical potential calculated using the van der Waals theory for (*A*) weak attraction, $\epsilon_{rr} = 2\epsilon^*_{rr}/3$, and (*B*) strong attraction, $\epsilon_{rr} = 4\epsilon^*_{rr}/3$. In (*A*) the receptor density increases monotonically and continuously, whereas for strong attraction (*B*), the relation between chemical potential and density exhibits a "van der Waals" loop: a discontinuous jump in the density of the equilibrium phases at which the partial derivative in Eq. **4** diverges, resulting in a large increase in selectivity.

larger than the valency $k$ and is instead limited by the maximum number of receptor–receptor bonds below a particle (which is approximately $2k$ for the square lattice model).

Our findings are not expected to be significantly affected by kinetic and finite size constraints unless the receptor copy number per cell is very low. In a realistic biological system, a typical receptor density is on the order of $\sigma \sim 1/(50\ \text{nm})^2$ and diffusivity $D \sim \mu\text{m}^2/\text{s}$ (23). To create a cluster of $k$ receptors, we need to recruit from an area of size $k/\sigma$ and the timescale $\tau_k$ to assemble a cluster is estimated as the typical time to diffuse across this area, $\tau_k \sim k/(\sigma D)$. For the case presented in Figs. 2 and 3, we use valency $k = 16$ and the kinetic timescale is thus $\tau_k < 0.1$ s, which is faster than typical cellular processes such as endocytosis. However, in general for a cell with $N$ receptors, the selectivity is limited by the finite cell size, $\alpha_r < N$, and also by the kinetics of cluster formation. If the relevant downstream activation or endocytosis process occurs on a timescale $\tau_{\text{activate}}$, then the typical cluster size $\tilde{k}$ that can be attained (and thus the typical selectivity) is expected to be limited by $\alpha_r < \tilde{k} \sim \sigma D \tau_{\text{activate}}$.

## 3. General Statistical Mechanics Basis for Enhanced Selectivity

To demonstrate the generality of the proposed mechanism, we provide a theoretical argument how interreceptor attraction can drastically increase the selectivity and, at the same time, tune the threshold value for the response. We stress that the effect of receptor–receptor attractions on clustering and superselectivity does not depend on the microscopic details of the system under consideration, and thus illustrate this point using a general thermodynamic argument. Readers less interested in the statistical mechanics background may skip this section.

The physics of what is essentially a first-order phase transition implies that cluster formation or condensation would occur whenever the receptor concentration is above a critical threshold, and result in the separation of receptors into two phases of high and low concentration spanning the whole membrane. This bulk separation reduces the selectivity (dashed line in Fig. 2*C*) and would change the properties of the whole membrane, which seems undesirable compared to a contained, localized response. Instead, a multivalent binding vector can induce local clustering of receptors (Fig. 3), driving the local receptor concentration above the critical value, even when the bulk concentration on the membrane is well below critical.

The probability that a vector binds at a specific spot on the surface is a function of the number of bonds that can be formed. In turn, this number depends on the local receptor concentration $\sigma_L$. By local we mean the receptor concentration in the surface region proximal to the multivalent vector; see Fig. 1 for reference. When receptors are mobile, the local concentration will be different from the concentration in the bulk of the membrane away from the vector, $\sigma_{ub}$. Typically $\sigma_L > \sigma_{ub}$ because interactions with the binding ligands will favor receptor accumulation in the binding region. We consider the general case, $\theta = \theta(\sigma_L(\gamma), \gamma)$; a control parameter can affect the binding probability $\theta$ both directly and indirectly, through changing the local concentration of receptors. We can now rewrite Eq. **2** explicitly as:

$$\begin{aligned}\alpha(\gamma) &= \frac{\mathrm{d}\ln\theta}{\mathrm{d}\ln\gamma} \\ &= \frac{\partial\ln\theta}{\partial\ln\sigma_L}\frac{\partial\ln\sigma_L}{\partial\ln\gamma} + \left(\frac{\partial\ln\theta}{\partial\ln\gamma}\right)_{\sigma_L} \\ &\equiv \alpha(\sigma_L)\frac{\partial\ln\sigma_L}{\partial\ln\gamma} + \left(\frac{\partial\ln\theta}{\partial\ln\gamma}\right)_{\sigma_L}. \end{aligned} \quad [3]$$

In Eq. **3**, $\alpha(\sigma_L)$ measures the sensitivity of binding to changes in the *local* concentration of receptors.

For grafted receptors (that is, with no lateral mobility), $\sigma_L = \sigma_{ub} = \sigma$, and hence the term $\frac{\partial\ln\sigma_L}{\partial\ln\gamma} = 1$ if $\gamma = \sigma$ and zero otherwise (the second term drops out if $\gamma = \sigma$). In this case, not only multivalent binding becomes a necessary condition to achieve a sharp superselective response (9), but it can only be obtained in a narrow range of receptor densities determined by the number of ligands in contact with the cell membrane and by the ligand–receptor bond energy. Tuning the response would then require that the cells change the chemical nature of

the bond by using a different receptor or through a fine-tuned modification of the part of the receptor at the extra-cytosolic side of the membrane. In contrast, for mobile receptors, the local concentration of receptors is generally different from the bulk concentration and can be tuned by various parameters. In particular, in the vicinity of a "condensation" transition, where the number density of the receptors changes discontinuously, the variation of the local concentration with $\gamma$ in the binding region, $\frac{\partial \ln \sigma_L}{\partial \ln \gamma}$, may even diverge, implying that the variation of $\theta$ with $\gamma$ (Eq. **3**) can become very large. Crucially, because the receptor density in the binding region is larger than in the bulk membrane, such condensation can occur locally while receptors in the rest of the membrane remain in a homogeneous, lower–density state (Figs. 1 and 3*A*).

As an illustrative and important example already explored above, we here focus on the binding response to changes in receptor density, $\gamma = \sigma$. For a typical case where receptor density is low and the fraction of bound receptors is also low, we can approximate $\sigma \approx \exp(\beta\mu_r)$, where $\mu_r$ is the chemical potential of the receptors, $\beta = 1/(k_B T)$, and where we have ignored an unimportant constant; see Fig. 4 for a visual illustration. For this case, the adsorption probability $\theta$ depends on $\sigma$ only through $\sigma_L$, so the second term in the r.h.s of Eq. **3** is zero, and we obtain

$$\alpha(\sigma) = \alpha(\sigma_L)\left(\frac{\partial \ln \sigma_L}{\partial \ln \sigma}\right) \approx \alpha(\sigma_L)\left(\frac{\partial \ln \sigma_L}{\partial(\beta\mu_r)}\right) . \quad [4]$$

To understand the physical meaning of $\frac{\partial \ln \sigma_L}{\partial(\beta\mu_r)}$, it is useful to rewrite $\sigma_L$ as $\sigma_L = \langle N_L\rangle/A$, where $A$ is the area of the binding region, see Fig. 1, and $\langle N_L\rangle$ is the average number of receptors in that region. We can then use the statistical mechanics of a "grand-canonical" system to express $\partial\langle N_L\rangle/\partial(\beta\mu_r) = \langle N_L^2\rangle - \langle N_L\rangle^2$, and obtain:

$$\frac{\partial \ln \sigma_L}{\partial(\beta\mu_r)} = \frac{\langle N_L^2\rangle - \langle N_L\rangle^2}{\langle N_L\rangle} \propto \kappa_T , \quad [5]$$

where $\kappa_T$ is the so-called isothermal compressibility. Thus, Eq. **5** shows that the sensitivity to small changes in the bulk receptor concentration $\sigma$ can be strongly enhanced in the vicinity of a phase transition or critical point where fluctuations (and compressibility) diverge. Of course, the number fluctuations can only truly diverge in the thermodynamic limit, but in a finite system they will still manifest a strong spike. We can calculate $\frac{\partial \sigma_L}{\partial \beta\mu_r}$ using an analytical theory for the liquid–vapor transition, such as the van der Waals theory illustrated in Fig. 4. Crucially, however, the details of the model do not matter: Eqs. **3–5** show that any model that predicts a condensation transition exhibits a large enhancement of the selectivity $\alpha$ as the attraction strength exceeds a threshold value. Of course, the exact values of the attraction strength and the density threshold needed to induce condensation of $\sigma_L$ are system-dependent. In the system explored above using the lattice model (Figs. 2 and 3), the selectivity indeed demonstrates a large increase when the membrane receptors are close to the condensation transition. It is important to stress that the condensation of receptors is limited to the binding region where the attraction between the multivalent particle and receptors tips the local receptors' density above the critical value.

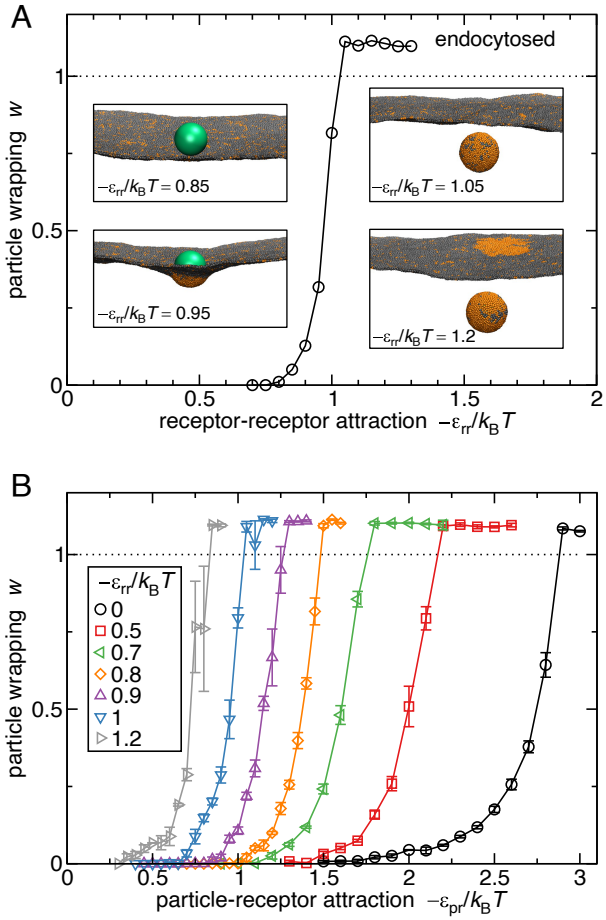


**Fig. 5.** Controlling endocytosis via receptor–receptor interaction $\varepsilon_{rr}$. (*A*) Particle wrapping dependence on $\varepsilon_{rr}$ at fixed particle–receptor interaction $\varepsilon_{pr} = -1\, k_BT$. *Insets* show final, stable configurations of the particle (green) and the membrane with lipids (gray) and receptors (orange). (*B*) Particle wrapping as a function of particle–receptor interaction $\varepsilon_{pr}$. Parameters: particle size $R_p = 8a$. Error bars show SEs, in (*A*) errors are smaller than the symbol size.

## 4. Receptor-Mediated Endocytosis

The effect of receptor attraction on selectivity is not limited to membrane binding. To demonstrate the relevance of above theory to general receptor-mediated processes, we consider the effect of interreceptor attraction on the wrapping and subsequent endocytosis of an extracellular cargo particle. The mechanism of cargo uptake has been extensively studied both experimentally (24–27) and with numerical modeling (28–33). Here, we consider a coarse-grained model of a flexible membrane with embedded receptors (34, 35). This model can reproduce both the fluidity and the elasticity of a membrane, yet it is simple enough to study the length and time scales relevant for receptor clustering and nano-particle endocytosis. The model also captures the required topological changes to the membrane, namely membrane pinch-off at the end of endocytosis, though the model does not explicitly model specific proteins that participate in the pinch-off process. We assume that the membrane contains a mixture of "lipid" particles (90%) and "receptor" particles (10%) of size $a \sim 5$ nm (Fig. 5*A*). Receptors can bind to ligands on the cargo nanoparticle (radius $R_p$) with an interaction energy $\varepsilon_{pr}$, which leads to membrane wrapping and endocytosis for sufficiently strong $\varepsilon_{pr}$. In addition, there is a receptor–receptor attraction $\varepsilon_{rr}$. When $\varepsilon_{rr} = 0$ the

receptors are randomly dispersed in the membrane, while for sufficiently strong attraction, $\varepsilon_{rr}/k_BT < -1$, and at the specific receptor density employed in our simulations, the receptors are prone to aggregate. To gauge the binding response in a way that is relevant for endocytosis, we monitor the extent of wrapping $w$, defined as the area of the membrane in contact with the nanoparticle, normalized by the nanoparticle surface (see *Materials and Methods*, Eq. **24**).

We find that the degree of wrapping $w$ of the cargo particle is extremely sensitive to receptor–receptor interaction $\varepsilon_{rr}$ (Fig. 5*A*). Starting from nonattracting receptors and increasing attraction, wrapping increases with a very sharp transition from no-wrapping to full-wrapping at $\varepsilon_{rr} \approx -k_BT$: A change of as little as $0.2\,k_BT$ reliably switches from no particle wrapping ($w = 0$) to full endocytosis ($w \geq 1$). This switching occurs in the absence of any phase separation or condensation in the bulk membrane. In contrast, at strong interactions ($\varepsilon_{rr} \leq -1.2\,k_BT$), receptors phase-separate and form a distinct domain (Fig. 5 *A*, *Inset*).

To further highlight these points, in Fig. 5*B*, we show how the degree of wrapping also depends on another control parameter, the particle–receptor bond energy $\varepsilon_{pr}$, calculated for different receptor–receptor interaction strengths $\varepsilon_{rr}$. We notice two main features: The first is that the sharpest variation of $w$ with $\varepsilon_{pr}$ occurs when $-\varepsilon_{rr} \approx k_BT$. This value should not come as a surprise: It is close to the miscibility critical point, i.e., the critical interaction strength which can be estimated from van der Waals theory to be at $\varepsilon^*_{rr} = -9\,k_BT/8$ (*Materials and Methods*), or from hexagonal Ising model which yields a very similar number $\varepsilon^*_{rr} = -\ln(3)\,k_BT$. This observation strengthens our point that the general physics of condensation and critical fluctuations plays an important role in boosting the sharpness of receptor mediated processes.

The second important feature is that, while interreceptor attraction can sharpen the binding and clustering response, the strength of such attraction can also be used to tune its onset (Fig. 5*B*). Hence, our simulations suggest that by modulating the strength of the interreceptor attraction, cells can effectively control particles–induced clustering and their subsequent internalization. Crucially, this control occurs without the need to affect the thermodynamic stability of the membrane; in the absence of cargo particle, no phase separation, condensation, or raft formation occurs and the membrane remains in a homogeneous state. The sharpness of the response makes this process extremely selective to the specific ligand–receptor pair that can activate it. We stress that in general the onset of the jump in the binding response with respect to other control parameters such as the receptor concentration $\sigma$ or the density of ligands on the particle can be similarly tuned (*Materials and Methods*). Such control could be useful, for example, to activate a response only when ligands are presented at high concentration (e.g., on the surface of a virus) and thus selectively detect viral infections. Alternatively, ability to lower the response threshold could enable the cells to deactivate the response; a mechanism that might be useful to avoid allergic reactions.

Last, we hypothesize that interreceptor attraction could also tune the size-specificity of endocytosis. Receptor-mediated endocytosis exhibits a peak endocytosis rate at a specific particle size (29, 35), typically below 100 nm, due to trade-off between membrane bending and receptor depletion. Introducing receptor–receptor attraction is expected to increase the local receptor density in the contact area, thereby shifting this trade-off. We thus hypothesize that increasing receptor–receptor attraction would shift the peak endocytosis rate toward smaller particles.

## 5. Summary

Summarizing, we have investigated how receptor–receptor attraction, and their clustering on a membrane, couples with the binding and the endocytosis of multivalent vectors. For both processes, we find that the introduction of weak interreceptor attraction strongly increases the sensitivity of the binding response, and allows to tune the point in parameter space ($\varepsilon_{pr}$, $\sigma$, ...) where a jump in the binding occurs. Such tuning, for example, could be important in the context of the formation of an immunological synapse (36, 37). What happens inside the cell after receptor binding, for instance, allosteric changes (2, 6, 38), is beyond the scope of this work.

The observed sensitivity enhancement (and the possibility to tune the activation onset) is associated to a very general and robust thermodynamic property of gas–liquid phase transitions: the discontinuity in the equilibrium density between the two phases. We thus expect it to play a potential role in a variety of systems where receptor–receptor interactions occur. We stress that the membrane should remain in a homogeneous state, since the occurrence of phase separation without the presence of a multivalent vector strongly reduces the selectivity. The relevance of our findings is enhanced by the wide body of work indicating that cell membranes operate close to a thermodynamic critical point (39).

As explained in ref. 6, there are many ways in which interreceptor attractions can be tuned, for example phosphorylation (3). Some, but not all, of these tuning mechanisms rely on intracellular processes. Our findings suggest how regulating such attraction could be used by cells to enhance or suppress the binding and potential uptake of external particles, be they natural or synthetic. Finally, we find it tempting to speculate that the immune system may tune interreceptor attraction to activate/deactivate immune cells (e.g. B-cells). A mechanism to detect dangerous from nondangerous entity must be "activated"—trigger a subsequent downstream response—when external ligands are presented above a threshold density (40). It is recognized that such activation often requires the clustering of receptors (41). The present paper suggests that, in particular for multivalent external particles, control of the interreceptor attraction provides a mechanism to tune and sharpen the activation response. This mechanism could also be employed to tune and enhance the selectivity of biosensors that either rely on multiple simultaneous bonds between "receptors" and the analyte of interest, or where the binding of the analyte enhances or suppresses the clustering of receptors.

## 6. Materials and Methods

**6.1. Monte Carlo Simulations.** The lattice model (Fig. 2*B*) contains a receptor layer in the membrane and a particle layer above it. Multivalent particles can adsorb to the membrane, without overlapping with each other, and bind to the receptors with interaction energy $\varepsilon_{pr}$. The multivalent particle describes, e.g., a ligand decorated nanoparticle (9) or a protein binding to specific membrane lipids (21). Likewise, "receptors" in our model refer to binding partners and can represent biological receptors or individual lipids.

The model contains two lattices and is described by five system parameters: The particle size and valency $k$ (i.e., the number of receptors a particle can bind to which determines the size ratio of the two lattices), particle chemical potential $\mu_p$, the receptor density $\sigma$, and two interaction energies: $\varepsilon_{rr}$, and

$\epsilon_{pr}$ (Fig. 2*B*). The potential energy $E$ of this system is given by the lattice gas Hamiltonian and a coupling term,

$$E = \epsilon_{rr} \sum_{<i,j>} s_i^r s_j^r + \epsilon_{pr} \sum_{i=1}^{M} s_i s_i^r \qquad [6]$$

where $s_i$ and $s_i^r$ are indicator functions specifying, respectively, whether a particle and a receptor are present ($s_i = 1$) or absent ($s_i = 0$) at a specific site $i$, and $< i, j >$ denotes nearest neighbor pairs. Thus, the first term takes into account receptor–receptor interactions and the second term the particle–receptor interactions. To investigate this system we employ grand-canonical Monte Carlo simulations and calculate $\langle N_p \rangle$, the average number of particles bound to the membrane (i.e., attached to at least one receptor). The system size $M = L^2$ with linear size $L = 80$ lattice sites, each receptor occupies one lattice site ($b = 1$) and particle size is a 4 x 4 square, $k = 16$. The receptors move on a $M = 80 \times 80$ lattice, while the top lattice consists of $M_p = 20 \times 20$ lattice sites with each top site overlapping with $k$ small lattice sites of the receptors. Both nanoparticles and receptors move freely but cannot overlap within their respective lattices. (Fig. 3). Periodic boundary conditions are applied to both lattices.

We employ grand-canonical Monte Carlo sampling of this system. The number of receptors is fixed by the receptor density, while the number of guests fluctuates and its average is determined by the chemical potential of the guest nanoparticles. Each simulation cycle employs three types of MC moves: i) move receptors, ii) move nanoparticles, and iii) insert/delete nanoparticles. In each cycle, we perform $\sigma M$ receptor move attempts, $\theta M/k$ guest move attempts, and one particle exchange move. The probability of adding a guest particle is:

$$\Pi_{N \to N+1} = \min\left[1, \frac{M}{(N+1)k} e^{\beta\mu_p} e^{-\beta(E_{N+1} - E_N)}\right] \qquad [7]$$

and to remove a particle is:

$$\Pi_{N \to N-1} = \min\left[1, \frac{Nk}{M} e^{-\beta\mu_p} e^{-\beta(E_{N-1} - E_N)}\right], \qquad [8]$$

where $\mu_p$ is the chemical potential of the particles and $E_N$ is the energy of the configuration with $N$ particles given by Eq. **6** The simulation consists of two major steps: equilibration and calculation. For the systems that have low receptor densities ($\sigma \leq 10^{-0.9}$), $10^7$ cycles were used for equilibration, while for the systems with higher receptor densities, $10^6$ cycles were used for equilibration, which was sufficient for the system energy to equilibrate. $10^8$ cycles were used for calculating $\theta$.

**6.2. Multivalent Lattice Theory.** In the absence of receptor–receptor interactions ($\epsilon_{rr} = 0$) the equilibrium $\theta$ can be approximated analytically. The partition function of a single particle $\xi_b$ that is attached to at least one receptor takes into account all possible binding states with the receptors. Since $\epsilon_{rr} = 0$, the receptor binding is uncorrelated each of the $k$ sites below a particle can be independently free or occupied by a receptor (35),

$$\xi_b = \left[1 + e^{\beta(\mu_r - \epsilon_{pr})}\right]^k - 1\,, \qquad [9]$$

where $\beta = 1/(k_B T)$ is the inverse temperature. The receptor chemical potential $\mu_r$ is determined by the density of unbound receptors $\sigma_{ub}$ (16),

$$e^{\beta\mu_r} = \frac{\sigma_{ub}}{1 - \sigma_{ub}}\,. \qquad [10]$$

The partition function of the same membrane section without a particle present is $\xi_u = \left(1 + e^{\beta\mu_r}\right)^k$, which evaluates to $\xi_u = (1 - \sigma_{ub})^{-k}$ using Eq. **10**. The free energy $F_{bond}$ due to bond formation of binding a particle to a specific surface site is thus

$$e^{-\beta F_{bond}} = \xi_b/\xi_u = \left[1 - \sigma_{ub} + \sigma_{ub} e^{-\beta\epsilon_{pr}}\right]^k - [1 - \sigma_{ub}]^k\,. \qquad [11]$$

Note that the dependence on the local receptor density $\sigma_L$ (that is, in the region below the particle; see Fig. 1) is implicit. Since $\sigma_L = \exp[\beta(\mu_r - \epsilon_{pr})]/(1 + \exp[\beta(\mu_r - \epsilon_{pr})])$, we can rewrite the above equation in terms of $\sigma_L$, instead of $\sigma_{ub}$,

$$e^{-\beta F_{bond}} = \left[1 - \sigma_L + \sigma_L e^{\beta\epsilon_{pr}}\right]^{-k} \left(1 - [1 - \sigma_L^k]\right)\,. \qquad [12]$$

For attractive ligand–receptor interaction $\beta\epsilon_{pr} < 0$, Eq. **12** is a monotonically increasing function of $\sigma_L$.

In the absence of particle–particle interactions (except for excluded volume) we can consider the standard Langmuir adsorption model and assume that there are $M_p$ independent binding sites for particles,

$$\theta = \frac{z e^{-\beta F_{bond}}}{1 + z e^{-\beta F_{bond}}}, \qquad [13]$$

where the activity $z = \exp(\beta\mu_p)$. In the dilute limit is $z = \rho v_0$, with $\rho$ being the number density of the particles in solution and $v_0$ the binding volume, see e.g., ref. 10 for a detailed description. Since $\sigma_{ub}$ depends on the number of adsorbed particles, determining the particle coverage $\theta$, in general, requires numerically finding a self-consistent solution (42). However, at low particle coverage where only a fraction of receptors is bound, we can approximate $\sigma_{ub} \approx \sigma$ and the guest particle coverage $\theta$ is determined analytically via Eq. **11**. This theory is in excellent agreement with MC data (Fig. 2) for $\sigma \ll \theta$ at which the approximation $\sigma_{ub} \approx \sigma$ is applicable.

If strong receptor–receptor interactions exist and receptor density is low we can consider all-or-nothing binding, i.e., the leading term in Eq. **11** dominates,

$$e^{-\beta F_{bond}} (\beta\epsilon_{rr} \ll -1) \approx \left[\sigma e^{-\beta(\epsilon_{pr} + z\epsilon_{rr}/2)}\right]^k\,, \qquad [14]$$

where $z$ is the average number of neighbors per receptor and thus we have added the effective contribution per receptor $z\epsilon_{rr}/2$. Using Eqs. **1** and **13**, we can easily show that the maximum selectivity $\alpha_r \to k$.

**6.3. A Minimal Model of Binding Enhancement via Receptor–Receptor Attraction.** We derive an approximate theory considering the effect of nonzero receptor–receptor interaction $\epsilon_{rr}$. If the ligand density on the particle is higher than that of the surface receptors, then the ligand–receptor binding free energy per receptor area, $f_{bond}(\sigma_L)$ is a monotonically decreasing function of the local density of receptors $\sigma_L$ in the binding region (9, 17), that is, the region between the multivalent vector and the surface of the membrane where ligand–receptor bonds can form; see Fig. 1 for clarity. A step change in the receptor density in the binding region corresponds to a step decrease in free energy, which in turn can translate into a step increase in binding probability. If this finite change occurs upon an infinitesimal change in a control parameter, it would manifest itself as a divergence in the derivative of $\gamma$ (Eq. **3** in the main text), in other words, infinite selectivity $\alpha$.

We now describe a simple model for the total free energy of the system to show under which conditions such divergence should be expected. We highlight that the model simplicity is meant to illustrate what are the minimal features required, thus actually encompassing a large variety of more complex models. As in the main text, the receptor–receptor attraction is controlled by the energy parameter $\epsilon_{rr}$. To keep the model to maximum simplicity, we describe the receptor free-energy density per unit area $f$ using a Van der Waals functional, plus an additional contribution due to bond formation in the binding region between the particle and the surface, that is:

$$f(\sigma) = k_B T \sigma \ln\left[\frac{\sigma/\sigma_0}{1 - b\sigma}\right] - k_B T \sigma - a_v \sigma^2 + f_{bond}(\sigma)\,, \qquad [15]$$

where $b$ and $a_v = -\epsilon_{rr} b$ are the standard van der Waals parameters specifying the excluded volume per receptor and interaction, respectively. $\sigma_0$ is the reference density that determines the reference value of the chemical potential. Without loss of generality we can set $\sigma_0 = 1$. $f_{bond}(\sigma)$ is the free-energy contribution due to ligand–receptor bond formation, which we stress once more is a local contribution present exclusively inside the binding region. For

simplicity, this region is defined as $r < R_p$, where $R_p$ is the radius of the particle, equivalent to the assumption that ligand–receptor bonds are much shorter than the size of the particle itself. We approximate $f_{bond}(\sigma)$ to be linear in $\sigma$ by considering that each receptor can independently bind to any of the $k$ ligands,

$$f_{bond}(\sigma) = \sigma \Delta G_{eff}, \quad [16]$$

where the effective free energy per receptor in the binding region is

$$\Delta G^{eff} = -k_B T \ln(1 + k \exp(-\beta \Delta G_{lr})), \quad [17]$$

with $k$ the average number of ligands interacting with the surface and $\Delta G_{lr}$ is the ligand–receptor bond energy. This approximation is accurate when the fraction of bound ligands is small, which is often the case for multivalent particles. Relaxing these conditions only complicates the mathematics without qualitatively changing any of the results we present. For example, to compare with the lattice theory above, $f_{bond} = F_{bond}/k$, since $F_{bond}$ is determined by particle of size $k$, while $f_{bond}$ is free energy per receptor area. Eq. **16** becomes equivalent to Eq. **12** in the limit of $\sigma \to 0$ and rescaling the bond energies, $\beta\epsilon_{pr} = -\ln(1 + \exp(-\beta \Delta G_{lr}))$, since, contrary to here, the lattice model considers all ligands below the particle to be bound.

Within the framework of classical density functional theory (43), we look for the receptor density field $\sigma(r)$, that minimizes the Grand Potential:

$$\gamma = \int_A [f(\sigma(r)) - \mu_r \sigma(r)] \, dr \,, \quad [18]$$

where $r$ is the position on the membrane of total area $A$. Minimization requires

$$\frac{\delta \gamma}{\delta \sigma(r)} = 0 \,, \quad [19]$$

which in our model leads to the simple Euler–Lagrange equation,

$$\frac{\partial f(\sigma)}{\partial \sigma(r)} = 0, \quad [20]$$

The solution to this problem leads to two equations for $\sigma_L$ and $\sigma_{ub}$, the receptor densities inside the local binding region (L) and on the bulk of the membrane (ub), respectively:

$$k_B T \ln\left[\frac{\sigma_L}{1 - b\sigma_L}\right] + k_B T \left[\frac{b\sigma_L}{1 - b\sigma_L}\right] - 2a_v \sigma_L + \Delta G_{eff} = \mu_r \,, \quad [21]$$

$$k_B T \ln\left[\frac{\sigma_{ub}}{1 - b\sigma_{ub}}\right] + k_B T \left[\frac{b\sigma_{ub}}{1 - b\sigma_{ub}}\right] - 2a_v \sigma_{ub} = \mu_r \,. \quad [22]$$

Note that as long as the density of receptors in the bulk of the membrane is low, $\sigma_{ub} \to 0$, we can approximate Eq. **22** as $\mu_r \approx k_B T \ln \sigma_{ub}$, so that fixing the average density in the membrane is equivalent to fixing the overall chemical potential. These equations can be solved with numerical methods to any desired accuracy. Additionally, for thermodynamic stability, only regions where the derivative of the chemical potential is positive correspond to minima of the Grand Potential and thus have a physical meaning, so we need to exclude intersections where this is not the case. Albeit shifted by a constant, $\Delta G_{eff}$, both inside and outside the binding region, the chemical potential takes the van der Waals form. From textbook thermodynamics (16), we know that the system will develop an instability, recognized as regions of negative slope, for $a_v \geq a^* = 9b\, k_B T/8$, or equivalently, $\epsilon_{rr}/\epsilon^*_{rr} \geq 1$ with $\epsilon^*_{rr} = -9\, k_B T/8$.

When an instability occurs a two-phase coexistence should be expected with a high and low density of receptors. The density jump leads to a discontinuity in the local density as a function of the chemical potential; see Fig. 5, which leads to a formally infinite superselectivity (Eq. **4**). We stress that although we chose the van-der-Walls form here, any model predicting a gas–liquid phase transition will necessarily show this qualitative behavior.

Having provided the qualitative description, we now numerically solve Eqs. **21** and **22** to find the equilibrium density of receptors in the binding region upon their condensation. Critically, this density is a function of the average density of receptors in the bulk membrane $\sigma_{ub}$ (i.e., receptors chemical potential), interreceptor attraction $\epsilon_{rr}$ and of the ligand–receptor effective bond

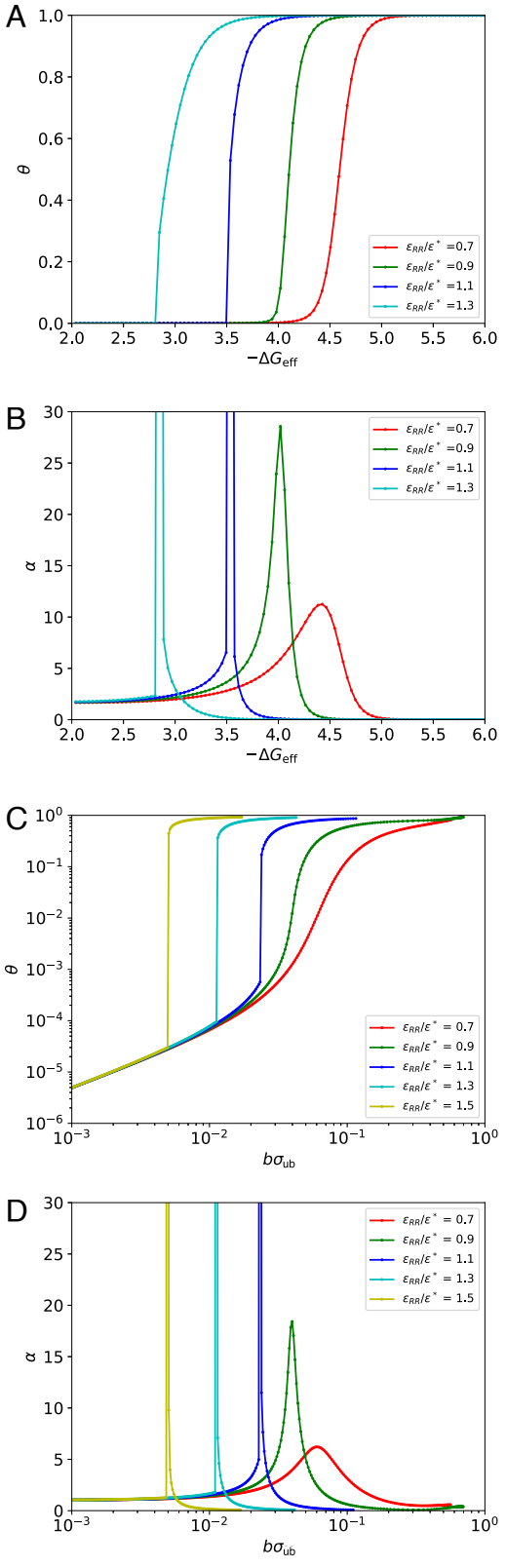


**Fig. 6.** Superselectivity from van der Waals theory. (*A* and *B*) Adsorption probability $\theta$ and the corresponding selectivity parameter $\alpha$ as a function of the effective bond energy (Eq. **17**) for various values of the receptor–receptor attraction $\epsilon_{rr}$ close to the critical value $\epsilon^*_{rr}$ at a fixed concentration of membrane receptors of $b\sigma_{ub} = 0.006$ and fixed particle activity $z = 10^{-4}$. (*C* and *D*) as in (*A* and *B*) but varying the concentration of receptors in the membrane $\sigma_{ub}$ at a fixed value of the receptor–receptor attraction $\Delta G_{eff} = -3\, k_B T$. Note how the adsorption can be tuned to jump at different values of $\Delta G_{eff}$ (i.e., different number of ligands, or ligand type) or $\sigma_{ub}$, and how the selectivity increases when approaching the critical state $\epsilon^*_{rr}$, and diverges when condensation is reached ($\alpha \to \infty$).

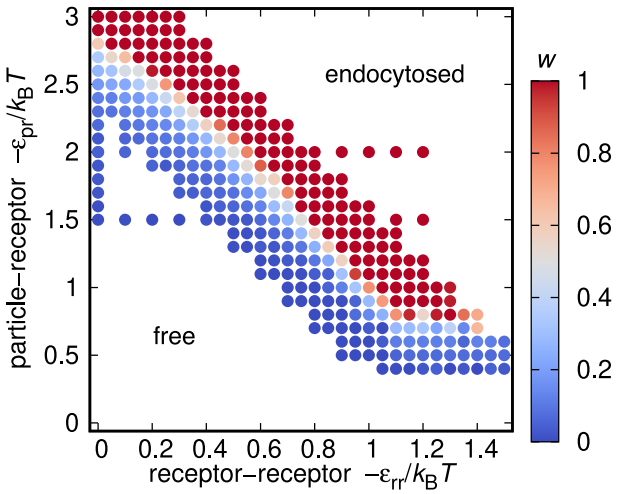


**Fig. 7.** Nanoparticle wrapping $w$ dependence on receptor–receptor and particle–receptor interaction energies.

energy $G_{lr}$. The obtained value is used to calculate the multivalent binding energy from Eq. **16** and thus the adsorption probability $\theta$ from Eq. **13** as well as the superselectivity $\alpha$ from Eq. **2**. The results of this procedure are plotted in Fig. 6.

This model effectively mirrors the key characteristics of the more intricate simulations discussed in the main body of the text: a sudden surge in binding probability and a marked rise in selectivity, contingent on various control parameters, with $\alpha$ nearing infinity whenever the system turns critical in the binding area. In this context, while a necessary condition for receptor condensation is a minimum value for their attraction (in this model, $\varepsilon_{rr} \to \varepsilon_{rr}^{*}$), it is crucial to note that even under such circumstances, condensation only takes place in the binding area when the local density of receptors approaches a certain value. This value is dependent on the effective ligand–receptor bond energy $\Delta G^{\text{eff}}$, the precise value of the receptor–receptor attraction $\varepsilon_{rr}$ and the overall density of receptors in the membrane. As previously discussed, the last two parameters can be internally regulated by a cell, either by producing more receptors or by employing adaptor proteins. Consequently, this mechanism enables cells to control activation, distinguishing between external particles with varying values of these attributes.

**6.4. Membrane Simulation Model.** The membrane is modeled using a coarse-grained one-particle thick model (34), implemented in the LAMMPS Molecular Dynamics package (44). In short, in this model, each membrane bead is described by its position and an axial vector. The beads interact with a combination of an attractive potential that depends on the interbead distance and drives the membrane self-assembly, and an angular potential that depends on the angle between the axial vectors of neighboring beads and mimics membrane bending rigidity. Following the notation from the original paper (34), we chose the parameters $\varepsilon_{\text{mem}} = 4.34\, k_BT$, $\xi = 4$, $\mu = 3$, $r_{\text{cut}}^{\text{bead}-\text{bead}} = 1.12\, a$, with $a$ the bead size, so that our membrane is in the fluid phase. Each membrane bead represents either a receptor or a lipid portion of the membrane. To investigate the role of receptor–receptor interactions, the interreceptor bead interaction strength $\varepsilon_{\text{rec}-\text{rec}} = \varepsilon_{\text{mem}} - \varepsilon_{rr}$, while the receptor–lipid interaction is the same as lipid–lipid interaction and given by $\varepsilon_{\text{mem}}$. Note, defined in this way, $\varepsilon_{rr}$ is the effective energy when two receptors are in contact.

The cargo nanoparticle interacts with the membrane via a cut and shifted Lennard-Jones potential,

$$U(r) = 4\varepsilon_{\text{LJ}}\left[\left(\frac{a}{r-R_p}\right)^{12} - \left(\frac{a}{r-R_p}\right)^{6}\right] + U_{\text{cs}}\,, \qquad [23]$$

for $0 \le r - R_p \le r_{\text{cut}}$ and $U(r) = 0$ otherwise. Here, $r$ is the bead to particle center-of-mass distance and $R_p$ is the nanoparticle radius. The interaction between the cargo and any of the nonreceptor beads is governed only by volume exclusion described by the Weeks–Chandler–Anderson potential, $U_{\text{cs}} = \varepsilon_{\text{WCA}}$ and $\varepsilon_{\text{LJ}} = \varepsilon_{\text{WCA}} = \varepsilon_{\text{mem}}$, $r_{\text{cut}} = 2^{1/6}\, a$. Conversely, the interaction between cargo and receptors is attractive: $r_{\text{cut}} = 2.6\, a$, $U_{\text{cs}}$ is set such that the potential is continuous at the cutoff, and $\varepsilon_{\text{LJ}} = -\varepsilon_{\text{pr}}$, which defines $\varepsilon_{\text{pr}}$ as the energy at contact analogous to the definition used in the lattice model.

We simulated a flat square portion of a membrane consisting of 49,920 beads with periodic boundary conditions in an $NpT$ ensemble with pressure $P = -10^{-4} k_BT/a^3$ to model a membrane with very low tension. The simulation box height was fixed at $L_z = 200\, a$. The surface tension of the membrane is therefore $\Pi = -pL_z = 2 \times 10^{-2}\, k_BT/a^2$. The component size of $a \approx 5$ nm results in $\Pi \approx 10^{-3}\, k_BT/\text{nm}^2$, which is at a lower end of biological surface tensions (30). The constant pressure is implemented via a Nosé–Hoover $NpH$ barostat. All the particles in the system are in addition subject to random noise implemented via a Langevin thermostat with friction coefficient set to unity: $\gamma = m/\tau$, where $m$ is the bead mass (set to unity) and $\tau$ the simulation unit of time. To capture the correct dynamics the cargo nanoparticle parameters are rescaled accordingly: mass of nanoparticle is $m_p = 8(R_p/a)^3$ and nanoparticle friction coefficient $\gamma_p = 2\, R_p/a$.

The initial condition of all simulations is a flat membrane with beads arranged on a hexagonal lattice and a randomly chosen permutation of bead identities (types) where a fraction 0.1 of beads are receptors and the rest are membrane beads. The location of the cargo particle's center of mass is a distance $R_p + 2a$ above the membrane. The endocytosis is monitored through the wrapping coverage of the cargo by the membrane beads, where the wrapping is defined as (35)

$$w = \frac{N^{\text{contact}}\sqrt{3}}{8\pi(R_p/a+1)^2}, \qquad [24]$$

with $N^{\text{contact}}$ being the number of membrane beads whose center-of-mass distance to the particle center is less than $R_p + a$. A nanoparticle is considered endocytosed if $w > 1$. The length of each simulation was $4 \times 10^7$ steps with a time step of $0.005\tau$. A final value of $w = w(\varepsilon_{rr}, \varepsilon_{pr})$ is shown in Fig 7, demonstrating that changing either $\varepsilon_{rr}$ or $\varepsilon_{pr}$ can be used to switch endocytosis on/off.

**Data, Materials, and Software Availability.** All study data are included in the main text.

**ACKNOWLEDGMENTS.** T.C. thanks Kalina Hristova for discussions and comments on the manuscript, and acknowledges support from the startup funds provided by the Whiting School of Engineering and the NSF, Division of Chemical, Bioengineering, Environmental and Transport Systems (CBET), Biosensors Program, Award Number 2402407. J.D. acknowledges support from the Chinese NSF through the Key research grant 12034019, and from the Strategic Priority Research Program of the Chinese Academy of Sciences through the grant XDB33000000. S.A.-U. and D.F. thank Clara Young, Christopher Goodnow, and Daniel Suan for illuminating discussions that helped framing this work within the context of the immune system.

1. T. D. Pollard, W. C. Earnshaw, J. Lippincott-Schwartz, G. Johnson, *Cell Biology E-Book: Cell Biology E-Book* (Elsevier Health Sciences, 2022).
2. T. Duke, D. Bray, Heightened sensitivity of a lattice of membrane receptors. *Proc. Natl. Acad. Sci. U.S.A.* **96**, 10104–10108 (1999).
3. C. C. Lin *et al.*, Receptor tyrosine kinases regulate signal transduction through a liquid-liquid phase separated state. *Mol. Cell.* **82**, 1089–1106.e12 (2022).
4. M. F. Sánchez, R. Tampé, Ligand-independent receptor clustering modulates transmembrane signaling: A new paradigm. *Trends Biochem. Sci.* **48**, 156–171 (2023).
5. P. Borowicz, H. Chan, A. Hauge, A. Spurkland, Adaptor proteins: Flexible and dynamic modulators of immune cell signalling. *Scand. J. Immunol.* **92**, e12951 (2020).
6. T. Duke, I. Graham, Equilibrium mechanisms of receptor clustering. *Prog. Biophys. Mol. Biol.* **100**, 18–24 (2009).
7. S. Banjade, M. K. Rosen, Phase transitions of multivalent proteins can promote clustering of membrane receptors. *eLife* **3**, e04123 (2014).
8. C. B. Carlson, P. Mowery, R. M. Owen, E. C. Dykhuizen, L. L. Kiessling, Selective tumor cell targeting using low-affinity, multivalent interactions. *ACS Chem. Biol.* **2**, 119–127 (2007).
9. F. J. Martinez-Veracoechea, D. Frenkel, Designing super selectivity in multivalent nano-particle binding. *Proc. Natl. Acad. Sci. U.S.A.* **108**, 10963–10968 (2011).
10. X. Tian, S. Angioletti-Uberti, G. Battaglia, On the design of precision nanomedicines. *Sci. Adv.* **6**, eaat0919 (2020).
11. G. V. Dubacheva, T. Curk, R. P. Richter, Determinants of superselectivity-practical concepts for application in biology and medicine. *Acc. Chem. Res.* **56**, 729–739 (2023).

12. N. M. English, J. F. Lesley, R. Hyman, Site-specific de-n-glycosylation of CD44 can activate hyaluronan binding, and CD44 activation states show distinct threshold densities for hyaluronan binding. *Cancer Res.* **58**, 3736–3742 (1998).
13. J. Wang, J. Min, S. A. Eghtesadi, R. S. Kane, A. Chilkoti, Quantitative study of the interaction of multivalent ligand-modified nanoparticles with breast cancer cells with tunable receptor density. *ACS Nano* **14**, 372–383 (2020).
14. M. S. Maginnis, Virus-receptor interactions: The key to cellular invasion. *J Mol. Biol.* **430**, 2590–2611 (2018).
15. J. Louten, *Essential Human Virology* (Academic Press, 2022).
16. R. Pathria, P. Beale, *Statistical Mechanics* (Elsevier Science, 2021).
17. M. Liu *et al*., Combinatorial entropy behaviour leads to range selective binding in ligand-receptor interactions. *Nat. Commun.* **11**, 4836 (2020).
18. A. Nohe, N. O. Petersen, Analyzing protein-protein interactions in cell membranes. *BioEssays* **26**, 196–203 (2004).
19. P. S. Niemelä, S. Ollila, M. T. Hyvönen, M. Karttunen, I. Vattulainen, Assessing the nature of lipid raft membranes. *PLoS Comput. Biol.* **3**, 1–9 (2007).
20. E. Sezgin, I. Levental, S. Mayor, C. Eggeling, The mystery of membrane organization: Composition, regulation and roles of lipid rafts. *Nat. Rev. Mol. Cell. Biol.* **18**, 361–374 (2017).
21. T. Curk, G. V. Dubacheva, A. R. Brisson, R. P. Richter, Controlling superselectivity of multivalent interactions with cofactors and competitors. *J. Am. Chem. Soc.* **144**, 17346–17350 (2022).
22. X. Xia, R. Ni, Designing superselectivity in linker-mediated multivalent nanoparticle adsorption. *Phys. Rev. Lett.* **132**, 118202 (2024).
23. Y. Gambin *et al*., Lateral mobility of proteins in liquid membranes revisited. *Proc. Natl. Acad. Sci. U.S.A.* **103**, 2098–2102 (2006).
24. J. J. Rennick, A. P. Johnston, R. G. Parton, Key principles and methods for studying the endocytosis of biological and nanoparticle therapeutics. *Nat. Nanotechnol.* **16**, 266–276 (2021).
25. T. G. Iversen, T. Skotland, K. Sandvig, Endocytosis and intracellular transport of nanoparticles: Present knowledge and need for future studies. *Nano Today* **6**, 176–185 (2011).
26. A. Akinc, G. Battaglia, Exploiting endocytosis for nanomedicines. *Cold Spring Harb. Perspect. Biol.* **5**, a016980 (2013).
27. W. Zhao *et al*., Nanoscale manipulation of membrane curvature for probing endocytosis in live cells. *Nat. Nanotechnol.* **12**, 750–756 (2017).
28. B. J. Reynwar *et al*., Aggregation and vesiculation of membrane proteins by curvature-mediated interactions. *Nature* **447**, 461–464 (2007).
29. H. Gao, W. Shi, L. B. Freund, Mechanics of receptor-mediated endocytosis. *Proc. Natl. Acad. Sci. U.S.A.* **102**, 9469–9474 (2005).
30. S. Zhang, J. Li, G. Lykotrafitis, G. Bao, S. Suresh, Size-dependent endocytosis of nanoparticles. *Adv. Mater.* **21**, 419–424 (2009).
31. R. Vácha, F. J. Martinez-Veracoechea, D. Frenkel, Receptor-mediated endocytosis of nanoparticles of various shapes. *Nano Lett.* **11**, 5391–5395 (2011).
32. A. H. Bahrami *et al*., Wrapping of nanoparticles by membranes. *Adv. Colloid Interface Sci.* **208**, 214–224 (2014).
33. J. Agudo-Canalejo, R. Lipowsky, Critical particle sizes for the engulfment of nanoparticles by membranes and vesicles with bilayer asymmetry. *ACS Nano* **9**, 3704–3720 (2015).
34. H. Yuan, C. Huang, J. Li, G. Lykotrafitis, S. Zhang, One-particle-thick, solvent-free, coarse-grained model for biological and biomimetic fluid membranes. *Phys. Rev. E* **82**, 011905-1-011905-8 (2010).
35. T. Curk, P. Wirnsberger, J. Dobnikar, D. Frenkel, A. Šarić, Controlling cargo trafficking in multicomponent membranes. *Nano Lett.* **18**, 5350–5356 (2018).
36. M. L. Dustin, A. K. Chakraborty, A. S. Shaw, Understanding the structure and function of the immunological synapse. *Cold Spring Harb. Perspect. Biol.* **2**, a002311 (2010).
37. B. Alarcón, D. Mestre, N. Martínez-Martín, The immunological synapse: A cause or consequence of T-cell receptor triggering? *Immunology* **133**, 420–425 (2011).
38. T. A. J. Duke, D. Bray, Heightened sensitivity of a lattice of membrane receptors. *Proc. Natl. Acad. Sci. U.S.A.* **96**, 10104–10108 (1999).
39. T. R. Shaw, S. Ghosh, S. L. Veatch, Critical phenomena in plasma membrane organization and function. *Annu. Rev. Phys. Chem.* **72**, 51–72 (2021).
40. W. E. Paul, *Fundamental Immunology* (Lippincott Williams & Wilkins, 2012).
41. D. Bray, M. D. Levin, C. J. Morton-Firth, Receptor clustering as a cellular mechanism to control sensitivity. *Nature* **393**, 85–88 (1998).
42. G. V. Dubacheva, T. Curk, D. Frenkel, R. P. Richter, Multivalent recognition at fluid surfaces: The interplay of receptor clustering and superselectivity. *J. Am. Chem. Soc.* **141**, 2577–2588 (2019).
43. R. Evans, The nature of the liquid-vapour interface and other topics in the statistical mechanics of non-uniform, classical fluids. *Adv. Phys.* **28**, 143–200 (1979).
44. A. P. Thompson *et al*., Lammps - a flexible simulation tool for particle-based materials modeling at the atomic, meso, and continuum scales. *Comput. Phys. Commun.* **271**, 108171 (2022).